

Neutron-pair transfer in the sub-barrier capture process

V. V. Sargsyan,^{1,2} G. Scamps,³ G. G. Adamian,¹ N. V. Antonenko,¹ and D. Lacroix⁴

¹Joint Institute for Nuclear Research, 141980 Dubna, Russia

²International Center for Advanced Studies, Yerevan State University, M. Manouagian 1, 0025 Yerevan, Armenia

³GANIL, 14076 Caen Cedex, France

⁴Institut de Physique Nucléaire, IN2P3-CNRS, Université Paris-Sud, F-91406 Orsay Cedex, France

(Received 27 October 2013; published 2 December 2013)

Sub-barrier capture reactions following neutron-pair transfer are proposed to be used for the indirect study of the neutron-neutron correlation in the surface region of a nucleus. The strong effect of dineutron-like cluster transfer stemming from the surface of magic and nonmagic nuclei ^{18}O , ^{48}Ca , ^{64}Ni , $^{94,96}\text{Mo}$, $^{100,102,104}\text{Ru}$, $^{104,106,108}\text{Pd}$, and $^{112,114,116,118,120,124,132}\text{Sn}$ is demonstrated. The dominance of the two-neutron transfer channel in the vicinity of the Coulomb barrier is further supported by time-dependent mean-field approaches.

DOI: [10.1103/PhysRevC.88.064601](https://doi.org/10.1103/PhysRevC.88.064601)

PACS number(s): 25.70.Jj, 24.10.-i, 24.60.-k

I. INTRODUCTION

Two-neutron transfer reactions such as (p, t) or (t, p) have been used for many years in order to study nucleon pairing correlations in stable nuclei [1,2]. The corresponding pair transfer modes are usually described in terms of pairing vibrations or pairing rotations [3,4], which are associated with the pair correlation. It has been established that the two-neutron transfer amplitude is influenced by collective modes caused by the Cooper-pair superfluidity [2]. In the superfluid nuclei ^{18}O , $^{206,210}\text{Pb}$, and ^{114}Sn , a Cooper pair with short-range space correlation has been theoretically predicted [5]. The size of the Cooper pair is estimated to be comparable to the average internucleon distance [5].

Recently, there has been a renewal of interest on experimental nucleon pairs, α clusters, and more generally multinucleon transfer channels at bombarding energies above and below the Coulomb barriers [6–8]. The effect of correlations between nucleons on the nuclear breakup or decay mechanism has been studied both experimentally and theoretically [9–14]. Studies of pairing effects in both finite nuclei and nuclear matter have intensified in recent years [15–26]. Attention has been paid to the properties of the pair correlation in neutron-rich nuclei with the neutron skin and the neutron halo [27–30]. The (p, t) reactions on light-mass neutron-rich nuclei such as $^6,8\text{He}$ and ^{11}Li point out the importance of the pair correlations in these typical halo or skin nuclei. The experimental signatures of a spatial two-neutron correlation or the dineutron correlation between two weakly bound neutrons forming the halo in $^6,8\text{He}$ and ^{11}Li have been reported in Refs. [31–35]. There exists also several studies demonstrating enhancement of the pair correlation in the nuclear surface and exterior regions of neutron-rich nuclei [18–21,23,36,37]. A possible link between pair transfer and the surface enhancement of the pairing in medium and heavy neutron-rich nuclei has been suggested in Ref. [38] and more recently discussed in [20–23,39]. It has been argued in Ref. [18] that pair transfer can be used as a possible probe of different models of the pairing interaction. In the literature [40], the origin of the small size of the Cooper pair on the nuclear surface is still under discussion. It can be a consequence of the enhanced pairing correlations or of the finiteness of the single-particle wave functions.

A strong spatial correlation between the nucleons gives rise to specific features such as dineutron or α clustering formation and to the possibility of a contribution to the transfer from the simultaneous one-step pair transfer mechanism. By describing the capture (fusion) reactions at sub-barrier energies within the quantum diffusion approach, we want to demonstrate indirectly the strong dineutron spatial correlations in the surface region of stable nuclei. We will consider capture reactions with negative one-neutron transfer ($Q_{1n} < 0$) and the positive two-neutron transfer ($Q_{2n} > 0$) (before crossing the Coulomb barrier), where the one-step neutron pair transfer is expected to be dominant. The study of this process is one of the important points in understanding pairing correlations in nuclei. The distinction between two-step sequential and one-step cluster transfer is a great challenge, not only in nuclear physics but also in electron transfer between ions or atomic cluster collisions [2]. Note that the capture (fusion) reaction following the neutron pair transfer is an indirect way of studying pairing effects.

II. MODEL

In the quantum diffusion approach [41–44] the collisions of nuclei are treated in terms of a single collective variable: the relative distance between the colliding nuclei. The nuclear deformation effects are taken into consideration through the dependence of the nucleus-nucleus potential on the deformations and mutual orientations of the colliding nuclei. Our approach takes into account the fluctuation and dissipation effects in the collisions of heavy ions which model the coupling with various channels (for example, coupling of the relative motion with the noncollective single-particle excitations and low-lying collective modes such as dynamical quadrupole and octupole excitations of the target and projectile [45]). We have to mention that many quantum-mechanical and non-Markovian effects accompanying the passage through the potential barrier are considered in our formalism [41,46] through friction and diffusion. Two-neutron transfer with a positive Q_{2n} value was taken into consideration in [41,43]. Our assumption is that, just before the projectile is captured by the target nucleus (i.e., just before the crossing of the Coulomb barrier), two-neutron

transfer occurs and can lead to the population of the first excited collective state in the recipient nucleus [7,47] (with the donor nucleus remaining in the ground state). So, the motion to the N/Z equilibrium starts in the system before the capture because it is energetically favorable in the dinuclear system in the vicinity of the Coulomb barrier. For the reactions under consideration, the average change of mass asymmetry is connected to the two-neutron transfer ($2n$ transfer). Since after the transfer the mass numbers, the isotopic composition, and the deformation parameters of the interacting nuclei, and, correspondingly, the height $V_b = V(R_b)$ (where $R = R_b$ is the position of the Coulomb barrier) and shape of the Coulomb barrier change, one can expect an enhancement or suppression of the capture. If after the neutron transfer the deformations of interacting nuclei increase (decrease), the capture probability increases (decreases). When the isotopic dependence of the nucleus-nucleus potential is weak and after the transfer the deformations of interacting nuclei do not change, there is no effect of the neutron transfer on the capture. In comparison with Ref. [48], we assume that the negative transfer Q values do not play a visible role in the capture process. Our scenario was verified in the description of many reactions [43]. The calculated results for all reactions are obtained with the same set of parameters as in Refs. [42,43] and are rather insensitive to a reasonable variation of them. One should note that the diffusion models, which include quantum statistical effects, were also treated in Refs. [49–51].

The capture cross section is the sum of the partial capture cross sections [41–43]:

$$\begin{aligned} \sigma_{\text{cap}}(E_{\text{c.m.}}) &= \sum_J \sigma_{\text{cap}}(E_{\text{c.m.}}, J) \\ &= \pi \lambda^2 \sum_J (2J+1) \int_0^{\pi/2} d\theta_1 \sin(\theta_1) \\ &\quad \times \int_0^{\pi/2} d\theta_2 \sin(\theta_2) P_{\text{cap}}(E_{\text{c.m.}}, J, \theta_1, \theta_2), \quad (1) \end{aligned}$$

where $\lambda^2 = \hbar^2/(2\mu E_{\text{c.m.}})$ is the reduced de Broglie wavelength, $\mu = m_0 A_1 A_2/(A_1 + A_2)$ is the reduced mass (where m_0 is the nucleon mass), and the summation is over the possible values of the angular momentum J at a given bombarding energy $E_{\text{c.m.}}$. Knowing the potential of the interacting nuclei for each orientation with the angles θ_i ($i = 1, 2$), one can obtain the partial capture probability P_{cap} , which is defined as the probability of penetrating the potential barrier in the relative distance coordinate R at a given J . The value of P_{cap} is obtained by integrating the propagator G from the initial state (R_0, P_0) at time $t = 0$ to the final state (R, P) at time t (where P is the momentum):

$$\begin{aligned} P_{\text{cap}} &= \lim_{t \rightarrow \infty} \int_{-\infty}^{r_{\text{in}}} dR \int_{-\infty}^{\infty} dP G(R, P, t | R_0, P_0, 0) \\ &= \lim_{t \rightarrow \infty} \frac{1}{2} \operatorname{erfc} \left[\frac{-r_{\text{in}} + \overline{R(t)}}{\sqrt{\Sigma_{RR}(t)}} \right]. \quad (2) \end{aligned}$$

Here, r_{in} is an internal turning point. The second line in (2) is obtained by using the propagator $G = \pi^{-1} |\det \Sigma^{-1}|^{1/2} \exp(-\mathbf{q}^T \Sigma^{-1} \mathbf{q})$ (where $\mathbf{q}^T =$

$[q_R, q_P], q_R(t) = R - \overline{R(t)}, q_P(t) = P - \overline{P(t)}, \overline{R(t=0)} = R_0, \overline{P(t=0)} = P_0, \Sigma_{kk'}(t) = 2q_k(t)q_{k'}(t)$, and $\Sigma_{kk'}(t=0) = 0, k, k' = R, P$) calculated for an inverted oscillator which approximates the nucleus-nucleus potential V in the variable R . At given $E_{\text{c.m.}}$ and J , the classical action is calculated for the realistic nucleus-nucleus potential. Then the realistic nucleus-nucleus potential is replaced by an inverted oscillator which has the same barrier height and classical action. So, the frequency $\omega(E_{\text{c.m.}}, J)$ of this oscillator is set to obtain an equality of the classical actions in the approximated and realistic potentials. The action is calculated in the WKB approximation, which is accurate at the sub-barrier energies. Usually in the literature the parabolic approximation with $E_{\text{c.m.}}$ -independent ω is employed but this is not accurate at deep sub-barrier energies. Our approximation is well justified for the reactions and energy range considered here [41–43]. Finally, one can find the expression for the capture probability:

$$P_{\text{cap}} = \frac{1}{2} \operatorname{erfc} \left[\left(\frac{\pi s_1 (\gamma - s_1)}{2\hbar\mu(\omega_0^2 - s_1^2)} \right)^{1/2} \frac{\mu\omega_0^2 R_0/s_1 + P_0}{[\gamma \ln(\gamma/s_1)]^{1/2}} \right], \quad (3)$$

where γ is the internal-excitation width, $\omega_0^2 = \omega^2 \{1 - \hbar\tilde{\lambda}\gamma/[\mu(s_1 + \gamma)(s_2 + \gamma)]\}$ is the renormalized frequency in the Markovian limit, and the value of $\tilde{\lambda}$ is related to the strength of linear coupling in the coordinates between collective and internal subsystems. Non-Markovian effects appear in the calculations through γ . Here, $\hbar\gamma = 15$ MeV. The s_i are the real roots ($s_1 \geq 0 > s_2 \geq s_3$) of the following equation [41–43]:

$$(s + \gamma)(s^2 - \omega_0^2) + \hbar\tilde{\lambda}\gamma s/\mu = 0. \quad (4)$$

As shown in Refs. [41,42], the nuclear forces start to play a role at $R_{\text{int}} = R_b + 1.1$ fm where the nucleon density of the colliding nuclei approximately reaches 10% of the saturation density. If the value of r_{ex} corresponding to the external turning point is larger than the interaction radius R_{int} , we take $R_0 = r_{\text{ex}}$ and $P_0 = 0$ in Eq. (3). For $r_{\text{ex}} < R_{\text{int}}$, it is natural to start our treatment with $R_0 = R_{\text{int}}$ and P_0 defined by the kinetic energy at $R = R_0$. In this case friction hinders the classical motion to proceed toward smaller values of R . If $P_0 = 0$ at $R_0 > R_{\text{int}}$, then friction almost does not play a role in the transition through the barrier. Thus, two regimes of interaction at sub-barrier energies differ by the action of the nuclear forces and the role of friction at $R = r_{\text{ex}}$.

To calculate the nucleus-nucleus interaction potential $V(R)$, we use the procedure described in Refs. [41–43,52]. For the nuclear part of the nucleus-nucleus potential, the double-folding formalism with the Skyrme-type density-dependent effective nucleon-nucleon interaction is used. The parameters of the potential were adjusted to describe the experimental data at energies above the Coulomb barrier corresponding to spherical nuclei. The absolute values of the quadrupole deformation parameters β_2 of even-even deformed nuclei and of the first excited collective states of nuclei were taken from Ref. [53]. For nuclei deformed in the ground state, β_2 in the first excited collective state is similar to β_2 in the ground state. For the double magic nuclei, we take $\beta_2 = 0$ in the ground state. For the rest of the nuclei, we used the ground-state quadrupole deformation parameters extracted in Ref. [43] from

a comparison of the calculated capture cross sections with the existing experimental data.

III. INFLUENCE OF NEUTRON-PAIR TRANSFER ON CAPTURE

The choice of the projectile-target combination is crucial in understanding the pair transfer phenomenon in the capture process. In capture reactions with $Q_{1n} < 0$ and $Q_{2n} > 0$, the two-step sequential transfer is almost closed before capture. So, by choosing properly the reaction combination, one can reduce the successive transfer in the process. For the systems studied, one can make unambiguous statements regarding the neutron transfer process with a positive Q_{2n} value when the interacting nuclei are double magic or semimagic nuclei. In this case one can disregard the strong nuclear deformation effects before the neutron transfer.

In Figs. 1 and 2 the calculated capture cross sections for the reactions $^{40}\text{Ca} + ^{48}\text{Ca}$ ($Q_{1n} = -1.6$ MeV, $Q_{2n} = 2.6$ MeV), $^{40}\text{Ca} + ^{116}\text{Sn}$ ($Q_{1n} = -1.2$ MeV, $Q_{2n} = 2.8$ MeV), $^{40}\text{Ca} + ^{124}\text{Sn}$ ($Q_{1n} = -0.1$ MeV, $Q_{2n} = 5.4$ MeV), $^{58}\text{Ni} + ^{64}\text{Ni}$ ($Q_{1n} = -0.66$ MeV, $Q_{2n} = 3.9$ MeV), and $^{64}\text{Ni} + ^{132}\text{Sn}$ ($Q_{1n} = -1.21$ MeV, $Q_{2n} = 2.5$ MeV) are in a good agreement with the available experimental data [54–57]. In all reactions $1n$ transfer is closed ($Q_{1n} < 0$) and Q_{2n} values for the $2n$

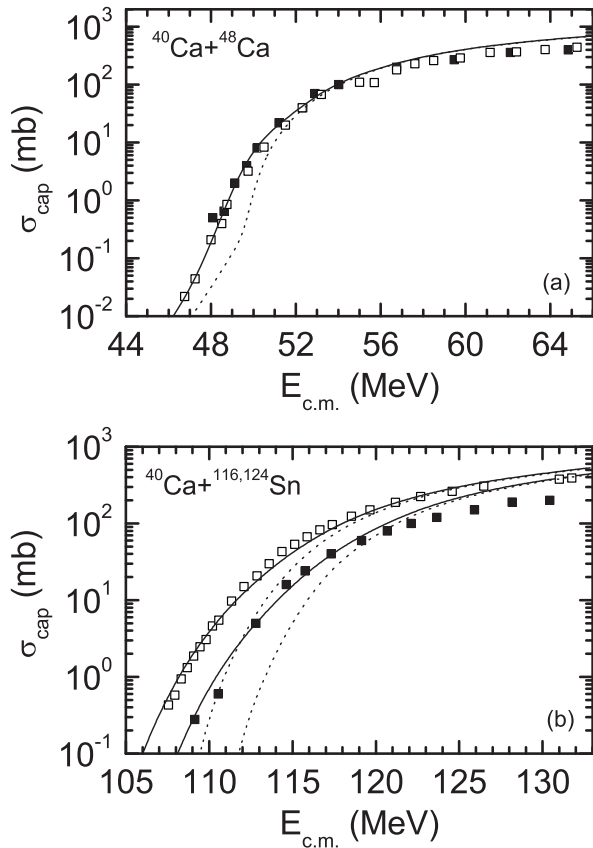


FIG. 1. The calculated (lines) and experimental (symbols) [54,55] capture cross sections vs $E_{\text{c.m.}}$ for the reactions $^{40}\text{Ca} + ^{48}\text{Ca}$ (a) and $^{40}\text{Ca} + ^{116,124}\text{Sn}$ (b). The calculated capture cross sections without taking into account neutron-pair transfer are shown by dotted lines.

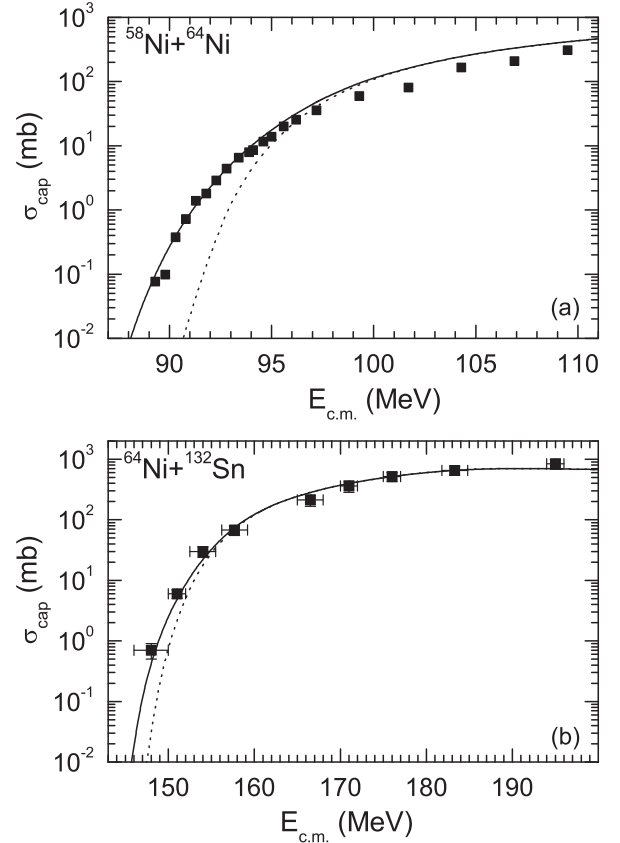


FIG. 2. The same as in Fig. 1, but for the reactions $^{58}\text{Ni} + ^{64}\text{Ni}$ (a) and $^{64}\text{Ni} + ^{132}\text{Sn}$ (b). The experimental data are from Refs. [56,57].

transfer processes are positive. Thus, the $2n$ transfer is more important for a good description of the experimental data than the $1n$ transfer. The influence of the $2n$ transfer on the capture cross section occurs due to the change of the isotopic composition and the deformations of the reaction partners. The $2n$ transfer indirectly influences the quadrupole deformation of the nuclei. When after neutron transfer (just before the crossing of the Coulomb barrier) in the reactions $^{40}\text{Ca}(\beta_2 = 0) + ^{48}\text{Ca}(\beta_2 = 0) \rightarrow ^{42}\text{Ca}(\beta_2 = 0.247) + ^{46}\text{Ca}(\beta_2 = 0)$, $^{40}\text{Ca}(\beta_2 = 0) + ^{116}\text{Sn}(\beta_2 = 0.112) \rightarrow ^{42}\text{Ca}(\beta_2 = 0.247) + ^{114}\text{Sn}(\beta_2 = 0.121)$, $^{40}\text{Ca}(\beta_2 = 0) + ^{124}\text{Sn}(\beta_2 = 0.095) \rightarrow ^{42}\text{Ca}(\beta_2 = 0.247) + ^{122}\text{Sn}(\beta_2 = 0.104)$, $^{58}\text{Ni}(\beta_2 = 0.05) + ^{64}\text{Ni}(\beta_2 = 0.087) \rightarrow ^{60}\text{Ni}(\beta_2 = 0.207) + ^{62}\text{Ni}(\beta_2 = 0.087)$, and $^{64}\text{Ni}(\beta_2 = 0.087) + ^{132}\text{Sn}(\beta_2 = 0) \rightarrow ^{66}\text{Ni}(\beta_2 = 0.158) + ^{130}\text{Sn}(\beta_2 = 0)$ the deformations of nuclei increase, the values of the corresponding Coulomb barriers decrease. As a result, two-neutron transfer enhances the capture process in these reactions at sub-barrier energies. The enhancement becomes stronger with decreasing bombarding energy (Figs. 1 and 2). Previously, the importance of neutron pair transfer in the capture (fusion) process was stressed in Refs. [48,58,59].

Since $Q_{1n} < 0$ in these reactions, the enhancement arises not from the coherent successive transfer of two single neutrons but from the direct transfer of one spatially correlated pair (the simultaneous transfer of two neutrons). Our results show that the capture (fusion) cross section of the reactions under consideration can be described by assuming preformed dineutron-like clusters in the ground state of the nuclei ^{48}Ca ,

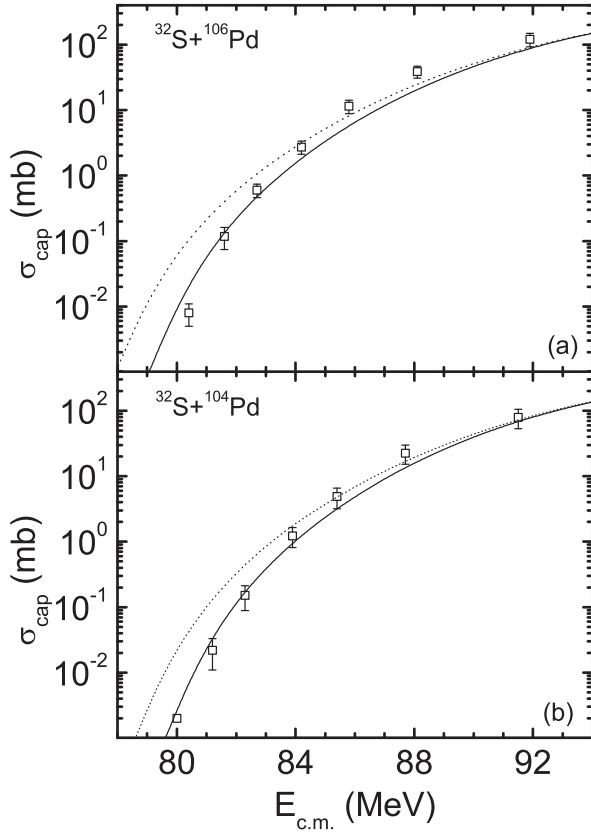


FIG. 3. The same as in Fig. 1, but for the reactions $^{32}\text{S} + ^{106}\text{Pd}$ (a) and $^{32}\text{S} + ^{104}\text{Pd}$ (b). The experimental data are from Ref. [58].

^{64}Ni , and $^{116,124,132}\text{Sn}$. Note that the strong spatial two-neutron correlation and the strong surface enhancement of the neutron pairing in the cases of a slab, semi-infinite nuclear matter, and finite superfluid nuclei are well known and it is well established that nuclear superfluidity of the Cooper pairs is mainly a surface effect [5,17,20].

Our calculations also show that neutron pair transfer has to be taken into consideration in the description of the reactions $^{58}\text{Ni} + ^{112,114,116,118,120}\text{Sn}$, $^{32}\text{S} + ^{94,96}\text{Mo}$, $^{100,102,104}\text{Ru}$, $^{104,106,108}\text{Pd}$, and $^{18}\text{O} + ^{112,118,124}\text{Sn}$ (for example, see Figs. 3 and 4) [43]. In Figs. 3 and 4 one can see that after neutron pair transfer in the reactions $^{32}\text{S}(\beta_2 = 0.312) + ^{106}\text{Pd}(\beta_2 = 0.229) \rightarrow ^{34}\text{S}(\beta_2 = 0.252) + ^{104}\text{Pd}(\beta_2 = 0.209)$, $^{32}\text{S}(\beta_2 = 0.312) + ^{104}\text{Pd}(\beta_2 = 0.209) \rightarrow ^{34}\text{S}(\beta_2 = 0.252) + ^{102}\text{Pd}(\beta_2 = 0.196)$ or $^{32}\text{S}(\beta_2 = 0.312) + ^{104}\text{Ru}(\beta_2 = 0.271) \rightarrow ^{34}\text{S}(\beta_2 = 0.252) + ^{102}\text{Ru}(\beta_2 = 0.24)$, $^{32}\text{S}(\beta_2 = 0.312) + ^{102}\text{Ru}(\beta_2 = 0.24) \rightarrow ^{34}\text{S}(\beta_2 = 0.252) + ^{100}\text{Ru}(\beta_2 = 0.215)$ the deformations of the nuclei decrease and the values of the corresponding Coulomb barriers increase and, respectively, the capture cross sections decrease at sub-barrier energies. These results indicate again the strong spatial two-neutron correlations in the surface of the stable nuclei ^{18}O , $^{94,96}\text{Mo}$, $^{100,102,104}\text{Ru}$, $^{104,106,108}\text{Pd}$, and $^{112,114,116,118,120}\text{Sn}$. Since the dominance of the dineutron-like clusters is found in the surface of double magic, semimagic, and nonmagic nuclei, one can conclude that this effect is general for all stable and radioactive nuclei.

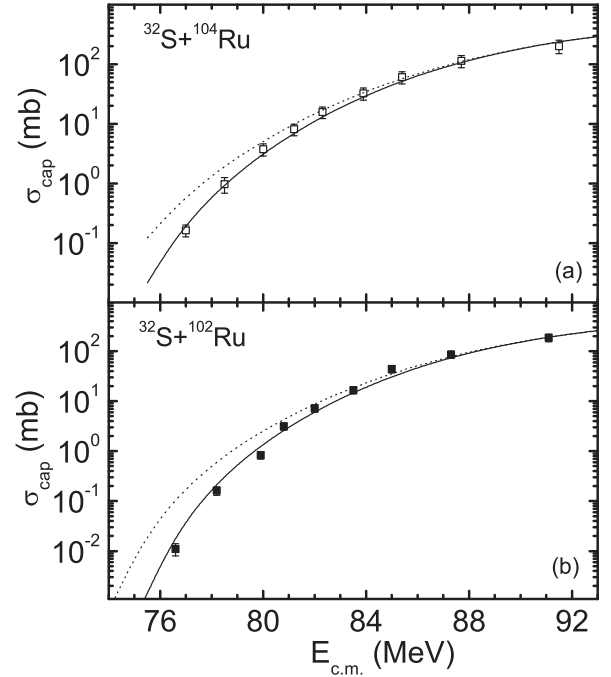


FIG. 4. The same as in Fig. 1, but for the reactions $^{32}\text{S} + ^{104}\text{Ru}$ (a) and $^{32}\text{S} + ^{102}\text{Ru}$ (b). The experimental data are from Ref. [58].

One can make unambiguous statements regarding the neutron pair transfer process in the reactions $^{40}\text{Ca} + ^{62}\text{Ni}$ ($Q_{1n} = -2.23$ MeV, $Q_{2n} = 1.43$ MeV), $^{40}\text{Ca} + ^{64}\text{Ni}$ ($Q_{1n} = -1.29$ MeV, $Q_{2n} = 3.45$ MeV), $^{40}\text{Ca} + ^{114}\text{Sn}$ ($Q_{1n} = -1.94$ MeV, $Q_{2n} = 1.8$ MeV), $^{40}\text{Ca} + ^{118}\text{Sn}$ ($Q_{1n} = -1.55$ MeV, $Q_{2n} = 3.56$ MeV), $^{40}\text{Ca} + ^{120}\text{Sn}$ ($Q_{1n} = -0.75$ MeV, $Q_{2n} = 4.25$ MeV), $^{40}\text{Ca} + ^{122}\text{Sn}$ ($Q_{1n} = -0.45$ MeV, $Q_{2n} = 4.86$ MeV), $^{58}\text{Ni} + ^{62}\text{Ni}$ ($Q_{1n} = -1.6$ MeV, $Q_{2n} = 1.94$ MeV), $^{60}\text{Ni} + ^{64}\text{Ni}$ ($Q_{1n} = -1.84$ MeV, $Q_{2n} = 1.95$ MeV), $^{64}\text{Ni} + ^{128}\text{Sn}$ ($Q_{1n} = -1.8$ MeV, $Q_{2n} = 1.6$ MeV), and $^{64}\text{Ni} + ^{130}\text{Sn}$ ($Q_{1n} = -1.52$ MeV, $Q_{2n} = 2.1$ MeV). As seen in Fig. 5, there is a considerable difference between the sub-barrier capture cross sections with and without taking into consideration neutron pair transfer in these reactions. After two-neutron transfer, the deformation of the light nucleus strongly increases and the capture cross section is enhanced. The neutron pair transfer induces quadrupole deformation in the light nucleus. The study of capture reactions following neutron transfer will provide a good test for the effects of neutron pair transfer.

IV. NEUTRON-PAIR TRANSFER IN HEAVY-ION SUB-BARRIER REACTIONS

The time-dependent Hartree-Fock (TDHF) plus BCS approach [60,61] has been recently used [61] to extract the one-, two-, and three-neutron transfer probabilities (P_{1n} , P_{2n} , and P_{3n}) in heavy-ion scattering reactions. It was shown that, when the energy is well below the Coulomb barrier, the one-nucleon channel largely dominates. This is further illustrated here for the reactions $^{40}\text{Ca} + ^{116,124,130}\text{Sn}$ that have been discussed above and where the tin isotopes are superfluid. In Fig. 6, the one- and two-neutron transfer probabilities are displayed as functions of $B_0 - E_{c.m.}$ for the sub- and near-barrier binary collisions of ^{40}Ca and tin isotopes. The Coulomb barrier

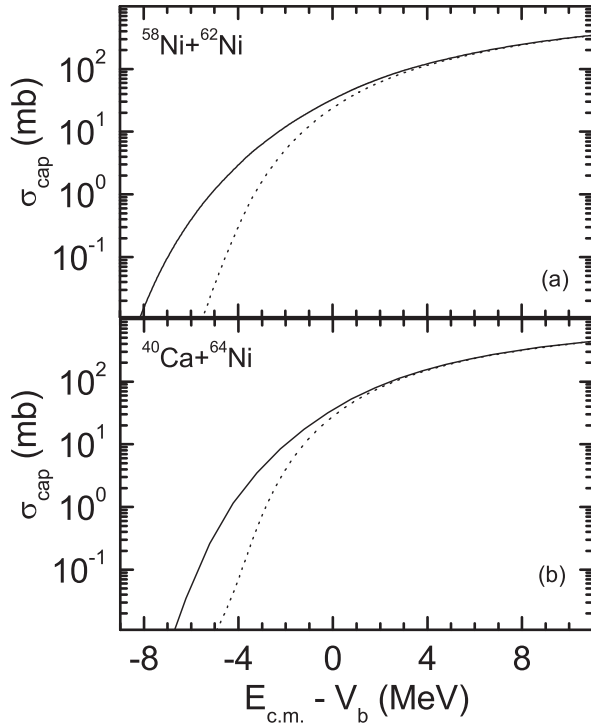


FIG. 5. The calculated capture cross section vs $E_{\text{c.m.}} - V_b$ for the reactions $^{58}\text{Ni} + ^{62}\text{Ni}$ (a) and $^{40}\text{Ca} + ^{64}\text{Ni}$ (b). The results with and without taking into consideration neutron-pair transfer are shown by solid and dotted lines, respectively.

(capture threshold energy) B_0 is deduced from the mean-field transport theory. This barrier are equal to 116.41 ± 0.07 (^{116}Sn), 114.69 ± 0.04 (^{124}Sn), and 113.92 ± 0.02 (^{130}Sn) MeV. It was found that the calculated B_0 values are insensitive to the introduction of pairing and in a good agreement with the barriers extracted from the experimental data [61]. Note that the presented calculations are shown for the mixed pairing interaction only. The use of other interactions (surface or volume) leads to similar conclusions. Figure 6 gives interesting

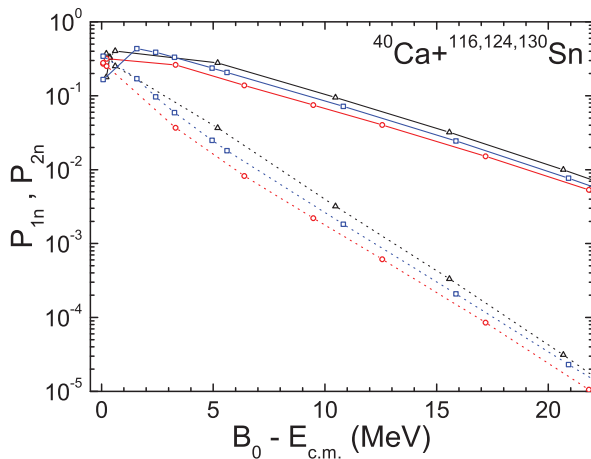


FIG. 6. (Color online) The calculated one-neutron (symbols connected by solid lines) and two-neutron (symbols connected by dotted lines) transfer probabilities vs $B_0 - E_{\text{c.m.}}$ for the reactions $^{40}\text{Ca} + ^{116}\text{Sn}$ (circles), $^{40}\text{Ca} + ^{124}\text{Sn}$ (triangles), and $^{40}\text{Ca} + ^{130}\text{Sn}$ (squares).

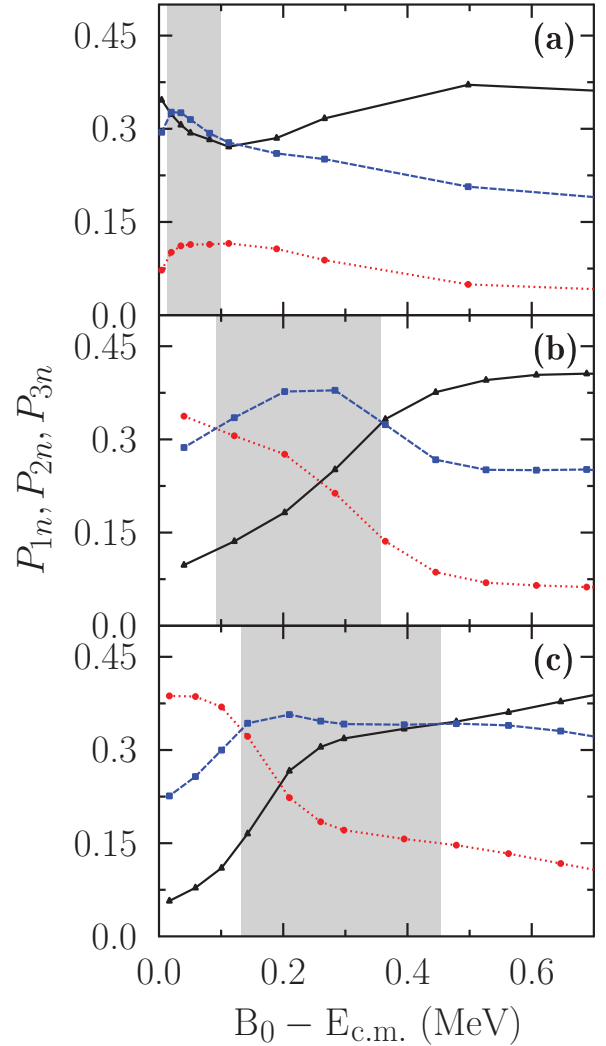


FIG. 7. (Color online) Closeup of the calculated one-neutron (black filled triangles), two-neutron (blue filled squares), and three-neutron (red filled circles) transfer probabilities as a function of $B_0 - E_{\text{c.m.}}$ for the reactions $^{40}\text{Ca} + ^{116}\text{Sn}$ (a), $^{40}\text{Ca} + ^{124}\text{Sn}$ (b), and $^{40}\text{Ca} + ^{130}\text{Sn}$ (c). In each case, the gray area indicates the energy region where the two-particle channel dominates.

insight into the one- and two-neutron transfers. As seen, a strong enhancement of P_{1n} and P_{2n} occurs with increasing bombarding energy. Since the enhancement of P_{2n} is stronger than that of P_{1n} , these probabilities become close to each other with decreasing $B_0 - E_{\text{c.m.}}$. This is indeed observed experimentally in Refs. [6–8], where it was found that P_{2n} grows faster than P_{1n} with decreasing $B_0 - E_{\text{c.m.}}$ at energy relatively far below the Coulomb barrier.

In Fig. 7, a closer look is taken at the one-, two- and three-neutrons transfer channels in the vicinity of the Coulomb barrier for the different tin isotopes. In all cases, as the energy approaches the capture barrier energy, there exists an energy range where $P_{2n} > P_{1n}$ dominates (shaded area). We also note that the energy windows where the two-nucleon channel becomes dominant increases as the neutron nucleus becomes more exotic.

This evidently supports our assumption about the important role of two-neutron transfer (compared to one-neutron transfer) in the capture process, because in the TDHF calculation the scattering trajectory of two heavy ions at energy near the Coulomb barrier is close to the capture trajectory. Note that in the capture process the system trajectory crosses the barrier position $R = R_b$ at any energy. The results of our calculations predict that there is a crossing point of P_{2n} and P_{1n} at energy very close to the Coulomb barrier. Just before reaching R_b the neutron-pair transfer becomes the dominant channel. Thus, our assumption about two-neutron transfer before the capture is correct. The transfer of more than two neutrons mainly occurs at $R < R_b$, i.e., just after the capture.

V. SUMMARY

Within the quantum diffusion approach it turns out that the sub-barrier capture (fusion) reactions with $Q_{1n} < 0$ and $Q_{2n} > 0$ may help us to understand neutron pair transfer and the pair correlation phenomenon on the surface of a nucleus. In these reactions the main contribution to transfer is due to the dineutron-like cluster component. In the capture process, the transfer of a neutron pair before the crossing of the Coulomb barrier is a clear signature of the strong correlations between the transferred nucleons and the surface character of the pairing interaction. Our results indicate

the dominance of the dineutron structure (of the preformed dineutron-like clusters) in the surface of the stable and unstable nuclei ^{18}O , ^{48}Ca , ^{64}Ni , $^{94,96}\text{Mo}$, $^{100,102,104}\text{Ru}$, $^{104,106,108}\text{Pd}$, and $^{112,114,116,118,120,124,132}\text{Sn}$. Measurements of sub-barrier capture cross sections in various reactions can be utilized to study the role of pairing correlations between the transferred nucleons. The information obtained from the sub-barrier capture (fusion) reactions is complementary to that obtained from two-neutron transfer reactions such as (p, t) or (t, p) and from multinucleon transfer reactions.

Employing the TDHF plus BCS approach [61], we demonstrated the important role of the two-neutron transfer channel in heavy-ion scattering at sub-barrier energies close to the Coulomb barrier. We suggest the experiments using $^{40}\text{Ca} + ^{116,124}\text{Sn}$ and $^{40}\text{Ca} + ^{48}\text{Ca}$ to check our predictions.

ACKNOWLEDGMENTS

We thank R. V. Jolos and H. Q. Zhang for fruitful discussions and suggestions. This work was supported by DFG and RFBR (Grants No. 12-02-31355, No. 13-02-12168, No. 13-02-000080, and No. 12-02-91159). The IN2P3(France)–JINR(Dubna) and Polish–JINR(Dubna) Cooperation Programmes are gratefully acknowledged.

-
- [1] O. Nathan and A. Bohr, in *Nuclear Structure: Dubna Symposium 1968* (International Atomic Energy Agency, Vienna, 1968).
- [2] W. von Oertzen and A. Vitturi, *Rep. Prog. Phys.* **64**, 1247 (2001).
- [3] D. R. Bes and R. A. Broglia, *Nucl. Phys.* **80**, 289 (1966); R. A. Broglia, O. Hansen, and C. Riedel, *Adv. Nucl. Phys.* **6**, 287 (1973).
- [4] R. V. Jolos, V. G. Kartavenko, F. Dönau, and D. Janssen, *Theor. Math. Fys.* **14**, 70 (1973); R. V. Jolos and V. G. Kartavenko, *Yad. Fys.* **19**, 964 (1974); *Theor. Math. Phys.* **20**, 353 (1974); R. V. Jolos, V. G. Kartavenko, and S. M. Semenov, *Yad. Fys.* **22**, 1121 (1975).
- [5] R. H. Ibarra, N. Austern, M. Vallieres, and D. H. Feng, *Nucl. Phys. A* **288**, 397 (1977); F. Catara, A. Insolia, E. Maglione, and A. Vitturi, *Phys. Rev. C* **29**, 1091 (1984); L. Ferreira, R. Liotta, E. H. Dasso, R. A. Broglia, and A. Winther, *Nucl. Phys. A* **426**, 276 (1984); M. A. Tischler, A. Tonina, and G. G. Dussel, *Phys. Rev. C* **58**, 2591 (1998).
- [6] L. Corradi, G. Pollarolo, and S. Szilner, *J. Phys. G* **36**, 113101 (2009).
- [7] L. Corradi *et al.*, *Phys. Rev. C* **84**, 034603 (2011).
- [8] M. Evers, M. Dasgupta, D. J. Hinde, D. H. Luong, R. Rafiei, R. du Rietz, and C. Simenel, *Phys. Rev. C* **84**, 054614 (2011).
- [9] F. M. Marqués *et al.*, *Phys. Rev. C* **64**, 061301(R) (2001).
- [10] J. J. Kolata *et al.*, *Phys. Rev. C* **75**, 031302 (2007).
- [11] S. N. Ershov and B. V. Danilin, *Phys. Part. Nucl.* **39**, 1623 (2008).
- [12] M. Assié and D. Lacroix, *Phys. Rev. Lett.* **102**, 202501 (2009); J. A. Scarpaci *et al.*, *Phys. Rev. C* **82**, 031301(R) (2010).
- [13] L. V. Grigorenko, I. G. Mukha, C. Scheidenberger, and M. V. Zhukov, *Phys. Rev. C* **84**, 021303(R) (2011).
- [14] A. Spyrou *et al.*, *Phys. Rev. Lett.* **108**, 102501 (2012).
- [15] L. Fortunato, W. von Oertzen, H. M. Sofia, and A. Vitturi, *Eur. Phys. J. A* **14**, 37 (2002).
- [16] A. Volya, V. Zelevinsky, and B. A. Brown, *Phys. Rev. C* **65**, 054312 (2002).
- [17] D. J. Dean and M. Hjorth-Jensen, *Rev. Mod. Phys.* **75**, 607 (2003).
- [18] E. Khan, N. Sandulescu, N. V. Giai, and M. Grasso, *Phys. Rev. C* **69**, 014314 (2004).
- [19] M. Baldo, U. Lombardo, E. E. Saperstein, and M. V. Zverev, *Phys. Rep.* **391**, 261 (2004).
- [20] M. Matsuo, K. Mizuyama, and Y. Serizawa, *Phys. Rev. C* **71**, 064326 (2005); M. Matsuo and Y. Serizawa, *ibid.* **82**, 024318 (2010); H. Shimoyama and M. Matsuo, *ibid.* **84**, 044317 (2011).
- [21] E. Pllumbi, M. Grasso, D. Beaumel, E. Khan, J. Margueron, and J. van de Wiele, *Phys. Rev. C* **83**, 034613 (2011).
- [22] G. Potel, F. Barranco, F. Marini, A. Idini, E. Vigezzi, and R. A. Broglia, *Phys. Rev. Lett.* **107**, 092501 (2011).
- [23] M. Grasso, D. Lacroix, and A. Vitturi, *Phys. Rev. C* **85**, 034317 (2012).
- [24] G. Scamps, D. Lacroix, G. F. Bertsch, and K. Washiyama, *Phys. Rev. C* **85**, 034328 (2012).
- [25] D. Gambacurta and D. Lacroix, *Phys. Rev. C* **86**, 064320 (2012).
- [26] M. Sambataro, *Phys. Rev. C* **85**, 064326 (2012).
- [27] M. V. Zhukov, B. V. Danilin, D. V. Fedorov, J. M. Bang, I. J. Thompson, and J. S. Vaagen, *Phys. Rep.* **231**, 151 (1993).
- [28] F. M. Marqués *et al.*, *Phys. Lett. B* **476**, 219 (2000).
- [29] F. Barranco, P. F. Bortignon, R. A. Broglia, G. Coló, and E. Vigezzi, *Eur. Phys. J. A* **11**, 385 (2001); E. Vigezzi, F. Barranco, R. A. Broglia, G. Coló, G. Gori, and F. Ramponi, *Nucl. Phys. A* **752**, 600 (2005).
- [30] M. Matsuo, *Phys. Rev. C* **73**, 044309 (2006).
- [31] G. M. Ter-Akopian *et al.*, *Phys. Lett. B* **426**, 251 (1998).

- [32] P. A. DeYoung *et al.*, *Phys. Rev. C* **71**, 051601 (2005).
- [33] T. Nakamura *et al.*, *Phys. Rev. Lett.* **96**, 252502 (2006).
- [34] P. Mueller *et al.*, *Phys. Rev. Lett.* **99**, 252501 (2007).
- [35] A. Chatterjee *et al.*, *Phys. Rev. Lett.* **101**, 032701 (2008).
- [36] E. E. Saperstein and M. V. Troitsky, *Yad. Fiz.* **1**, 10 (1965).
- [37] K. Hagino and H. Sagawa, *Phys. Rev. C* **72**, 044321 (2005).
- [38] J. Dobaczewski, W. Nazarewicz, T. R. Werner, J. F. Berger, C. R. Chinn, and J. Dechargé, *Phys. Rev. C* **53**, 2809 (1996).
- [39] M. Grasso, *Phys. Rev. C* **87**, 064308 (2013).
- [40] N. Pillet, N. Sandulescu, and P. Schuck, *Phys. Rev. C* **76**, 024310 (2007); N. Pillet, N. Sandulescu, P. Schuck, and J.-F. Berger, *ibid.* **81**, 034307 (2010); X. Viñas, P. Schuck, and N. Pillet, *ibid.* **82**, 034314 (2010).
- [41] V. V. Sargsyan, G. G. Adamian, N. V. Antonenko, and W. Scheid, *Eur. Phys. J. A* **45**, 125 (2010).
- [42] V. V. Sargsyan, G. G. Adamian, N. V. Antonenko, W. Scheid, and H. Q. Zhang, *Eur. Phys. J. A* **47**, 38 (2011); *J. Phys.: Conf. Ser.* **282**, 012001 (2011); *EPJ Web Conf.* **17**, 04003 (2011).
- [43] V. V. Sargsyan, G. G. Adamian, N. V. Antonenko, W. Scheid, and H. Q. Zhang, *Phys. Phys. C* **84**, 064614 (2011); **85**, 024616 (2012); **85**, 069903(E) (2012).
- [44] V. V. Sargsyan, G. G. Adamian, N. V. Antonenko, W. Scheid, C. J. Lin, and H. Q. Zhang, *Phys. Phys. C* **85**, 017603 (2012); V. V. Sargsyan, G. G. Adamian, N. V. Antonenko, W. Scheid, and H. Q. Zhang, *ibid.* **85**, 037602 (2012); R. A. Kuzyakin, V. V. Sargsyan, G. G. Adamian, N. V. Antonenko, E. E. Saperstein, and S. V. Tolokonnikov, *ibid.* **85**, 034612 (2012).
- [45] S. Ayik, B. Yilmaz, and D. Lacroix, *Phys. Rev. C* **81**, 034605 (2010).
- [46] V. V. Sargsyan, Z. Kanokov, G. G. Adamian, N. V. Antonenko, and W. Scheid, *Phys. Rev. C* **80**, 034606 (2009); V. V. Sargsyan, G. G. Adamian, N. V. Antonenko, W. Scheid, and H. Q. Zhang, *ibid.* **80**, 047603 (2009); V. V. Sargsyan, Z. Kanokov, G. G. Adamian, and N. V. Antonenko, *Part. Nucl.* **41**, 175 (2010).
- [47] S. Szilner *et al.*, *Phys. Rev. C* **84**, 014325 (2011).
- [48] R. A. Broglia, C. H. Dasso, S. Landowne, and A. Winther, *Phys. Rev. C* **27**, 2433 (1983); R. A. Broglia, C. H. Dasso, S. Landowne, and G. Pollarolo, *Phys. Lett. B* **133**, 34 (1983); C. H. Dasso, S. Landowne, and A. Winther, *Nucl. Phys. A* **405**, 381 (1983).
- [49] H. Hofmann, *Phys. Rep.* **284**, 137 (1997).
- [50] L. F. Canto, *Nucl. Phys. A* **491**, 337 (1989); N. Takigawa, S. Ayik, K. Washiyama, and S. Kimura, *Phys. Rev. C* **69**, 054605 (2004); S. Ayik, B. Yilmaz, A. Gokalp, O. Yilmaz, and N. Takigawa, *ibid.* **71**, 054611 (2005).
- [51] G. Hupin and D. Lacroix, *Phys. Rev. C* **81**, 014609 (2010).
- [52] G. G. Adamian, N. V. Antonenko, and W. Scheid, in *Clusters in Nuclei*, Vol. 2, edited by C. Beck, Lecture Notes in Physics (Springer-Verlag, Berlin, 2012), Vol. 848, p. 165.
- [53] S. Raman, C. W. Nestor, Jr., and P. Tikkanen, *At. Data Nucl. Data Tables* **78**, 1 (2001).
- [54] H. A. Aljuwair, R. J. Ledoux, M. Beckerman, S. B. Gazes, J. Wiggins, E. R. Cosman, R. R. Betts, S. Saini, and O. Hansen, *Phys. Rev. C* **30**, 1223 (1984); C. L. Jiang *et al.*, *ibid.* **82**, 041601(R) (2010).
- [55] F. Scarlassara, S. Beghini, G. Montagnoli, G. F. Segato, D. Ackermann, L. Corradi, C. J. Lin, A. M. Stefanini, and L. F. Zheng, *Nucl. Phys. A* **672**, 99 (2000).
- [56] J. F. Liang, D. Shapira, C. J. Gross, R. L. Varner, J. R. Beene, P. E. Mueller, and D. W. Stracener, *Phys. Rev. C* **78**, 047601 (2008).
- [57] M. Beckerman, M. Salomaa, A. Sperduto, J. D. Molitoris, and A. DiRienzo, *Phys. Rev. C* **25**, 837 (1982).
- [58] R. Pengo, D. Evers, K. E. G. Löbner, U. Quade, K. Rudolph, S. J. Skorka, and I. Weidl, *Nucl. Phys. A* **411**, 255 (1983).
- [59] A. M. Stefanini *et al.*, *Nucl. Phys. A* **456**, 509 (1986); A. M. Borges, C. P. da Silva, D. Pereira, L. C. Chamon, E. S. Rossi, Jr., and C. E. Aguiar, *Phys. Rev. C* **46**, 2360 (1992); S. Kalkal *et al.*, *ibid.* **83**, 054607 (2011).
- [60] C. Simenel and B. Avez, *Int. J. Mod. Phys. E* **17**, 31 (2008); C. Simenel, in *Clusters in Nuclei*, Vol. 3, edited by C. Beck, Lecture Notes in Physics (Springer-Verlag, Berlin, 2013), Vol. 875, p. 95.
- [61] G. Scamps and D. Lacroix, *Phys. Rev. C* **87**, 014605 (2013).